Generation of Counterpropagating Path-Entangled Photon Pairs in a Single Periodic Waveguide

Sina Saravi,* Thomas Pertsch, and Frank Setzpfandt
Institute of Applied Physics, Abbe Center of Photonics, Friedrich Schiller University Jena, Albert-Einstein-Strasse 6, 07745 Jena, Germany
(Received 9 January 2017; published 3 May 2017)

We propose the use of nonlinear periodic waveguides for direct and fully integrated generation of counterpropagating photon pairs by spontaneous parametric down-conversion. Using the unique properties of Bloch modes in such periodic structures, we furthermore show that two counterpropagating phase-matching conditions can be fulfilled simultaneously, allowing for the generation of path-entangled Bell states in a single periodic waveguide. To demonstrate the feasibility of our proposal, we design a photonic crystal slab waveguide made of lithium niobate and numerically demonstrate Bell-state generation.

DOI: 10.1103/PhysRevLett.118.183603

Sources of photon pairs are an essential part of quantum communication and computation protocols [1] and integrated optical structures are the top candidate for practical large-scale implementation of such quantum protocols [2–4]. An efficient way of generating photon pairs at room temperature is through nonlinear interactions, e.g., spontaneous parametric down-conversion (SPDC) [5–12] and spontaneous four-wave mixing (SFWM) [13–18], mediated by $\chi^{(2)}$ and $\chi^{(3)}$ nonlinearities, respectively. Nanostructured waveguides and resonators [8–10,14–17] have already shown to be efficient platforms for such applications, as they can be integrated, have high nonlinear efficiencies and narrowband interactions, while offering a strong control over the biphoton state and its degrees of entanglement [19], allowing preparation of photon pairs in the state required for a certain quantum protocol [20,21].

Nanostructured photonic crystal slab waveguides (PCSWs) can enhance nonlinear interactions [22] through the use of slow light [23], which in turn has resulted in the realization of highly efficient sources of photon pairs [16,17]. Moreover, the Bloch modes of a periodic waveguide can have dramatically different dispersion relations compared to that of a bulk material. This has been used in 1D Bragg structures to overcome the phase-matching limitations in an isotropic material system [24,25] and to allow control over the spectral degree of entanglement without being limited by the material dispersion [26]. PCSWs are particularly promising from this aspect, as they allow for engineering the dispersion of the guided Bloch modes through fine changes in the structure [27], which consequently can offer a strong control of the properties of the generated biphoton states.

A unique property of periodic structures is the capability of supporting umklapp nonlinear processes [28], in which large phase mismatches can be compensated through the extra momentum introduced by the periodic lattice without the need for periodic poling. This has already been studied for backward second-harmonic generation in 2D photonic crystals [29]. Importantly, the ability to phase match to modes counterpropagating to the pump (P) makes the propagation direction available as an extra degree of freedom (DOF) for creating entanglement in single waveguides [9]. This capability of periodic waveguides, to the best of our knowledge, has not yet been exploited for creating photon pairs entangled in the path DOF [30], which is uniquely suited for qubit encoding in integrated optical platforms [30] and allows the implementation of complex quantum algorithms [31].

In this work, we show that the umklapp process combined with dispersion engineering can be used to reach the phase matching of a pump mode to several combinations of signal (S) and idler (I) modes with different propagation directions schematically depicted in Figs. 1(a)–1(c). This eventually allows full control over the path DOF of entangled biphoton states. Of special interest are configurations where one or both of the generated photons are counterpropagating to the pump beam, which are highly desirable but technologically challenging to realize. These processes result in a much

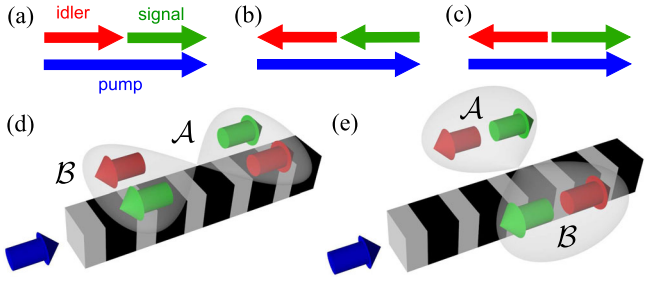

FIG. 1. Different phase-matching configurations, where with respect to a forward-propagating pump (a) both of the signal and idler photons are copropagating, (b) both are counterpropagating, (c) either signal or idler photon is counterpropagating; (d),(e) Scheme of different scenarios for creating path-entangled Bell states in a single periodic waveguide.

narrower spectrum [32,33], compared to the more common copropagating process, having the potential for reaching discrete-frequency entanglement [18,34]. They are also ideal for generation of factorizable pairs [20,35], uncorrelated in frequency, needed for realizing heralded single-photon sources. Moreover, counterpropagating configurations allow the splitting of the signal and idler photons from each other, like Fig. 1(c), or separating both signal and idler from the pump beam, like Fig. 1(b).

Building on the realization of one phase-matched counterpropagating process, we describe a general scheme for reaching simultaneous phase matching of several processes. As schematically depicted in Figs. 1(d), 1(e), this enables the completely integrated generation of path-entangled biphoton quantum states through SPDC in a single periodic waveguide with just one pump beam and without the need for periodic poling. To establish the practicality of our approach, we demonstrate the generation of the path-entangled Bell state of Fig. 1(e) with rigorous simulations of a lithium niobate ($LiNbO_3$) PCSW using its dispersion engineering capability.

The main challenge in realizing a counterpropagating SPDC configuration is satisfying the phase-matching condition, $k_P - k_S - k_I = 0$, for the wave vectors of the pump and the counterpropagating signal or idler waves. This can be achieved by periodic poling using either subwavelength poling periods, which are technologically challenging to achieve for optical wavelengths [36], or higher order poling, which results in much lower efficiencies [37]. Furthermore, pumping from above with a spatially broad free-space pump beam was used as a method to satisfy the phase-matching condition and experimentally demonstrated [9,32,33,38,39], but this is not compatible to a fully integrated platform. Finally, through SFWM, counterpropagating photon pairs could be created using two counterpropagating pump beams [40]; however, this approach cannot be transferred to SPDC.

We generate counterpropagating photon pairs in a completely integrated configuration using the properties of Bloch modes. We assume a periodic waveguide with periodicity a along the propagation direction x, and we take y and z to be the transversal directions along which exists a confinement mechanism. The electric field of a Bloch mode in such a structure can be described as $\boldsymbol{E}(\boldsymbol{r},\omega) = \boldsymbol{e}(\boldsymbol{r},\omega)\exp[ik(\omega)x] = \sum_{n=-\infty}^{+\infty} \boldsymbol{C}_n(y,z,\omega)\exp[ik_n(\omega)x]$, with $k_n(\omega) \equiv k(\omega) + 2\pi n/a$, where the periodic Bloch-mode profile $\boldsymbol{e}(\boldsymbol{r}) = \boldsymbol{e}(\boldsymbol{r} + a\hat{\mathbf{x}})$ is expanded in a Fourier series. This means a Bloch mode can be expanded into a series of x-invariant modes called Bloch harmonics (BHs) [28], described by $\boldsymbol{C}_n$. In an efficient nonlinear process, phase matching is required between BHs and consequently the phase-matching condition is $k_P = k_S + k_I + 2\pi(n_S + n_I - n_P)/a$ [28]. The efficiency of the process depends on how well the transverse field profiles of these BHs overlap and how strongly each BH contributes to its corresponding Bloch mode. Usually, the dominant BH of a forward-propagating (FWP) Bloch mode has a positive k_n, and its value is closer to the k of a corresponding FWP mode in an unstructured material than the k_n of weaker BHs. In previous works in 1D Bragg structures [24–26], only the dominant BHs were used for phase matching in an effort to maximize the efficiency of the process, which subsequently limits the designs to only copropagating configurations. However, for a FWP Bloch mode, the lower the group velocity $v_g = d\omega/dk$ of the mode gets, the higher the contribution of BHs with negative k_n becomes. As a result, by using slower modes, one can increase and even control the efficiency of processes that involve the nondominant BHs, which is the key for satisfying a counterpropagating phase-matching condition and also reaching a maximally entangled Bell state.

First, we explain the phase-matching scheme exemplarily for a counterpropagating process where S and I propagate in different directions. Consider the band diagrams shown in Figs. 2(a) and 2(b), which correspond to a realistic structure to generate the path-entangled state of Fig. 1(e), but can be viewed schematically at this stage. We first want to phase match process $\mathcal{A}$, involving three different modes, a FWP pump, a FWP signal, and a backward-propagating (BWP) idler. The BH distribution of these modes can be estimated by calculating the Fourier transform of the dominant E_y field component of the Bloch modes on the $y = z = 0$ line along the propagation direction, which are shown in Fig. 2(c). The magnitudes of the peaks correspond to $C_n = \hat{\mathbf{y}} \cdot \boldsymbol{C}_n(y = 0, z = 0)$. There are two relatively strong BHs for each of the S and I modes, as we chose both modes near the edge of the Brillouin zone (BZ). Of interest for us is the $C_{1,S}$ BH for the FWP signal with $k_{1,S} = k_{S,\mathrm{FW}} + 2\pi/a$ and the $C_{0,I}$ BH for the BWP idler with $k_{0,I} = k_{I,\mathrm{BW}}$. We use these two BHs to

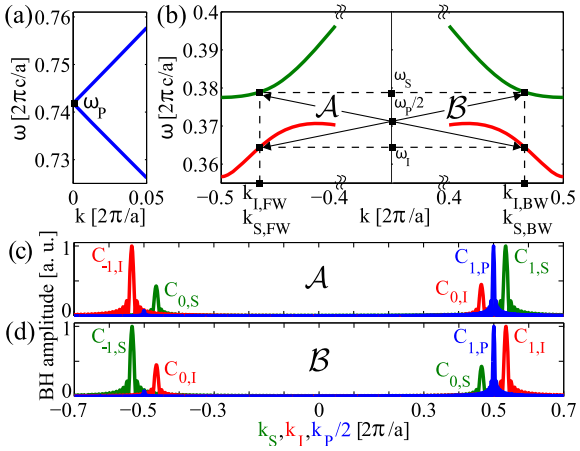

FIG. 2. (a) Band diagram of the pump mode; (b) Band diagram of the signal mode (green) and idler mode (red), explaining the condition for simultaneous phase-matching for processes $\mathcal{A}$ and $\mathcal{B}$ graphically, referring specifically to the path-entangled state of Fig. 1(e); Bloch-harmonic (BH) distribution for the modes involved in process $\mathcal{A}$ (c) and $\mathcal{B}$ (d).

phase match to the pump mode. We need the two $k_{S,\mathrm{FW}}$ and $k_{I,\mathrm{BW}}$ to have opposite signs, so that $k_{1,S} + k_{0,I} \approx 2\pi/a$. To achieve phase matching, we need a pump at the frequency of $\omega_P = \omega_S + \omega_I$ with a dominant BH around the k of $2\pi/a$, which translates to a $k \approx 0$ in the first BZ. $k \approx 2\pi/a$ for the dominant BH of the P mode is a physically achievable value for a mode around twice the frequency of the S and I modes, given that the S and I modes themselves have a k around π/a. The band diagram for such a P mode and its corresponding BHs are shown in Figs. 2(a) and 2(c), respectively, where we divided the k axis for the P mode by a factor of 2.

Importantly, satisfying the phase-matching condition is only based on the k values of the modes and their BHs, and does not depend on the group velocity $v_g = d\omega/dk$ of the signal and idler bands, whose signs determine the propagation direction. As a result, one can control the propagation direction of the generated photons by controlling the sign of the group velocity at the wave vectors of phase matching using dispersion engineering. Hence, SPDC processes with arbitrary combinations of the signal or idler propagation directions can be realized.

With the knowledge of how to phase match a single process, we move on to generate path-entangled biphoton states, for which simultaneous phase matching of at least two SPDC processes as described above is necessary. In reciprocal structures as considered here, this can be automatically achieved for processes which phase match two different S and I bands with a pump mode at $k_P = 0$. If process $\mathcal{A}$ in Fig. 2(b) is phase matched with $k_P = 0$, then process $\mathcal{B}$ is phase-matched likewise, but with switched propagation directions of the signal and idler photons. The following conditions are satisfied: $k_P = 0$, $k_{I,\mathrm{BW}} = k_{S,\mathrm{BW}} = -k_{S,\mathrm{FW}} = -k_{I,\mathrm{FW}}, \omega_P = \omega_{S_{\mathrm{FW}}} + \omega_{I_{\mathrm{BW}}} = \omega_{S_{\mathrm{BW}}} + \omega_{I_{\mathrm{FW}}}, \omega_{S_{\mathrm{FW}}} = \omega_{S_{\mathrm{BW}}}$, and $\omega_{I_{\mathrm{FW}}} = \omega_{I_{\mathrm{BW}}}$, all presented graphically in Fig. 2(b). To further illustrate the simultaneous phase matching, we plot the BH distributions of process $\mathcal{B}$ in Fig. 2(d). Under the above conditions, the BHs of the S and I modes simply exchange their places in the two processes, but since they are at the same k values, they phase match to the same FWP pump mode that has a dominant BH with $k_{1,P} = 2\pi/a$.

We calculate the path-entangled biphoton state (see Supplemental Material [41]) using a standard perturbative method [25,42], with a leaky classical P mode [43] and quantized lossless S and I modes [44]. The resulting biphoton state is

$$|\psi\rangle \propto \iint d\omega_S \quad d\omega_I \{\mathcal{A}(\omega_S,\omega_I)|S,\mathrm{FW},\omega_S\rangle|I,\mathrm{BW},\omega_I\rangle + \mathcal{B}(\omega_S,\omega_I)|S,\mathrm{BW},\omega_S\rangle|I,\mathrm{FW},\omega_I\rangle\}, \tag{1}$$

where $\mathcal{A}(\omega_S,\omega_I) = \sqrt{\omega_S\omega_I}\mathrm{Ov}_{\mathcal{A}}A_P(\omega_S+\omega_I)\mathrm{JPS}_{\mathcal{A}}$ is the joint spectral amplitude (JSA) for process $\mathcal{A}$, with the joint phase-matching spectrum (JPS) and overlap integral (Ov) defined as:

$$\mathrm{JPS}_{\mathcal{A}} \equiv \frac{e^{[i(k_P - k_{S,\mathrm{FW}} - k_{I,\mathrm{BW}}) - \alpha_P]L} - 1}{i(k_P - k_{S,\mathrm{FW}} - k_{I,\mathrm{BW}}) - \alpha_P}, \tag{2a}$$

$$\mathrm{Ov}_{\mathcal{A}} \equiv \frac{\sqrt{n_{g_S} n_{g_I}} \int_\Omega d^3\boldsymbol{r} \sum^{\alpha\beta\gamma} \chi^{(2)}_{\alpha\beta\gamma} e_{P,\gamma} e^*_{S,\mathrm{FW},\alpha} e^*_{I,\mathrm{BW},\beta}}{\sqrt{\int_\Omega d^3\boldsymbol{r} \boldsymbol{d}_S \boldsymbol{e}^*_S \int_\Omega d^3\boldsymbol{r} \boldsymbol{d}_I \boldsymbol{e}^*_I}}. \tag{2b}$$

For finding $\mathcal{B}(\omega_S,\omega_I)$, indices BW and FW should be exchanged, BW $\leftrightarrow$ FW. Variables with indices I, S, and P are functions of frequencies ω_I, ω_S, and $\omega_I + \omega_S$, respectively. Bloch-mode field profiles and $\chi^{(2)}$ are functions of $\boldsymbol{r}$. Here A_P is the frequency envelope of the pump pulse, n_g is the group index of a guided mode, $1/\alpha_P$ is the decay length of the leaky pump mode, $\boldsymbol{e}$ and $\boldsymbol{d}$ are the electric and displacement field profiles of the Bloch mode, respectively, Ω is the volume of a unit cell, and L is the length of the structure. The $|S/I,\mathrm{FW/BW},\omega_S/\omega_I\rangle$ is the single photon state at the frequency ω_S/ω_I in the signal (idler) mode propagating forward (backward). The generated biphoton state is entangled in 3 DOF of mode, frequency, and direction of propagation, although in this case the mode DOF is also a binary subspace of the frequency DOF.

To generate a maximally entangled Bell state in the path DOF, we must have the same nonlinear efficiency along with modal and spectral indistinguishability for processes $\mathcal{A}$ and $\mathcal{B}$. Modal indistinguishability is assured, as the FWP and BWP counterparts of the S and I modes in a reciprocal material are identical. For equal nonlinear efficiencies of processes $\mathcal{A}$ and $\mathcal{B}$ we need to satisfy $\alpha_{\mathcal{A}} = \alpha_{\mathcal{B}}$, with $\alpha_{\mathcal{A}} \equiv \int d\omega_S \int d\omega_I |\mathcal{A}(\omega_S,\omega_I)|^2$ and $\alpha_{\mathcal{B}} \equiv \int d\omega_S \int d\omega_I |\mathcal{B}(\omega_S,\omega_I)|^2$, which strongly depends on the overlap integral of Eq. 2(b). In order to have spectral indistinguishability, we need to satisfy $\alpha_{\mathcal{B}} = |\alpha_{\mathcal{AB}}|$, with $\alpha_{\mathcal{AB}} \equiv \int d\omega_S \int d\omega_I \mathcal{A}(\omega_S,\omega_I)\mathcal{B}^*(\omega_S,\omega_I)$, which ensures that the two JSAs have perfect spectral overlap, controlled by the pump spectrum and the JPS.

To show the feasibility of our approach for generating Bell states, we design a PCSW of $LiNbO_3$ suspended in air, which generates the maximally entangled state with antibunched signal and idler photons propagating in opposite directions, as shown in Fig. 1(e). The used double-slot structure is shown in Fig. 3 with the design parameters and field profiles of the modes involved. All modes are TE-like, with a dominant E_y component, and with the crystal axis along the y direction, the nonlinear interaction is dominantly mediated by the d_{33} coefficient of $LiNbO_3$'s nonlinear tensor. The corresponding band diagrams are shown in Figs. 2(a) and 2(b). The P mode is above the light line and leaky [43], whereas the S and I modes are in the band gap frequency region of the two-dimensional photonic crystal slab and under the light line of air and hence ideally lossless. Double-slot structures have previously been used for sensing applications [45]. Here we propose their use to reduce leakage radiation of the P mode. The slot

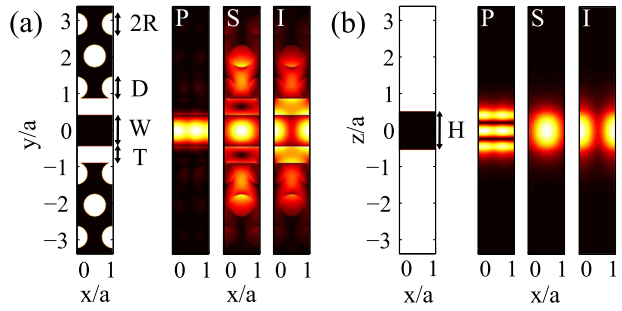

FIG. 3. Double-slot PCSW design, with a membrane of lithium niobate of thickness H, suspended in air ($R/a = 0.3$, $H/a = 1.07$, $W/a = 0.85$, $T/a = 0.45$, $D/a = 0.59$) with the Bloch-mode profile of the P, S, and I modes (E_y component) at planes (a) $z = 0$; (b) $y = 0$.

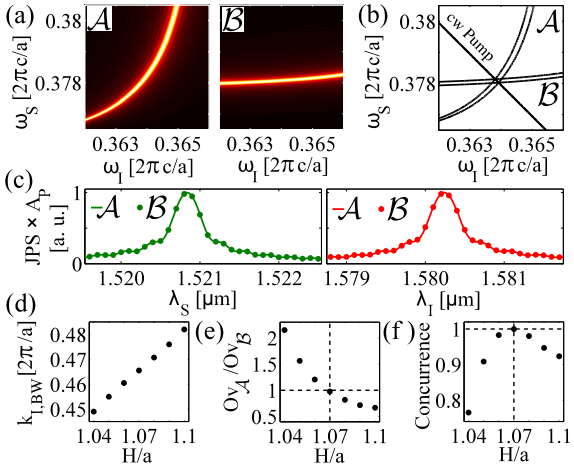

FIG. 4. (a) Joint phase-matching spectrum (JPS) of $\mathcal{A}$ and $\mathcal{B}$; (b) Overlap of JPSs with the cw pump line; (c) Projected spectrum of the S and I photons from both processes. Changes in design properties as a function of slab thickness H; (d) Wavevector $k_{I,\mathrm{BW}}$ at the central point of phase matching (according to Fig. 2); (e) Ratio between the efficiencies of processes $\mathcal{A}$ and $\mathcal{B}$; (f) Concurrence of the quantum state.

width T has to be large enough for the P mode to not interact with the photonic crystal slab that is responsible for the leakage. Simultaneously, T has to be small enough for the S and I modes, that are at lower frequencies and transversally broader, to couple to the photonic crystal slab, which allows for the dispersion engineering. In our specific design we have $T = 0.45a = 259$ nm, with $a = 575$ nm to set the pump wavelength at 0.775 μm. We note that this proposal could also open the way for efficient harmonic generation in PCSWs, which previously suffered from the high leakage of the higher-harmonic modes. We reach a decay length of about 447 periods or 257 μm, which is about an order of magnitude larger than what could usually be achieved for a similar higher order mode in a standard W1 PCSW [43]. Finally, we choose the structure length $L = 1000a = 575$ μm. Although both the efficiency and the spectral bandwidth of the nonlinear process tend to saturate for structure lengths larger than the decay length of the pump mode, the phase-matching spectrum approaches a Lorentzian function in this limit, in contrast to the sinc function of a lossless case, which is advantageous in increasing the similarity between the produced JSAs of both processes.

First, we demonstrate spectral overlap between processes $\mathcal{A}$ and $\mathcal{B}$. The corresponding JPSs are shown in Fig. 4(a). To achieve similar JSAs we use a continuous-wave (cw) pump at $\omega_P a/2\pi c = 0.742$ ($k_P = 0$), corresponding to the vacuum wavelength of 0.775 μm. The pump spectrum $A_P(\omega_S + \omega_I = 0.742)$ for this cw pump is a line, shown in Fig. 4(b) overlapped with the two JPSs. The fact that this line passes the JPSs exactly at their crossing point is a direct consequence of our simultaneous phase-matching design. This results in an almost perfect spectral overlap of $\mathcal{A}(\omega_S, \omega_I)$ and $\mathcal{B}(\omega_S, \omega_I)$. We show this overlap more clearly in Fig. 4(c), by plotting $\mathcal{A}(\omega_S, \omega_I)$ and $\mathcal{B}(\omega_S, \omega_I)$ projected onto each of the ω_S and ω_I axes, here presented as a function of wavelength. Although the SPDC bandwidth is limited by the pump decay, it is still much narrower compared to that of a copropagating phase-matching scheme in similarly short structures.

To design equal nonlinear efficiencies for processes $\mathcal{A}$ and $\mathcal{B}$, we have to calculate the overlap integral for both processes from Eq. 2(b). Given that the dominant BHs involved in phase-matching process $\mathcal{A}$ ($C_{1,S}$, $C_{0,I}$, and $C_{1,P}$), except for $C_{1,P}$, are different than those involved in process $\mathcal{B}$ ($C_{0,S}$, $C_{1,I}$, and $C_{1,P}$), we do not generally expect $\mathrm{Ov}_{\mathcal{A}} = \mathrm{Ov}_{\mathcal{B}}$. However, the distributions of Bloch harmonics of the S and I modes strongly depend on their wave vectors k. By changing the thickness of the slab H, we can control the wave vectors $k_{I,\mathrm{BW}} = k_{S,\mathrm{BW}}$ [see Fig. 2(b)] at which phase matching is achieved. The advantage of changing H in this design is that the shape of the S and I bands mostly depend on in-slab parameters and are not affected. Changing H will only shift these bands up and down in frequency, with stronger shifts for the P mode, which is a higher order mode in the z direction. To quantify the entanglement, we calculated the concurrence $\mathcal{C} \equiv 2|\alpha_{\mathcal{AB}}|/(\alpha_{\mathcal{A}} + \alpha_{\mathcal{B}})$ [9]. The changes in the phase-matching wave vector, the ratio $\mathrm{Ov}_{\mathcal{A}}/\mathrm{Ov}_{\mathcal{B}}$, and the calculated concurrence are shown in Figs. 4(d)–4(f). Equal efficiencies are reached for $H = 1.07a \approx 615$ nm, resulting in a concurrence of 1, which indicates the generation of a maximally entangled Bell state.

In summary, we proposed a general scheme for direct generation of counterpropagating photon pairs and path-entangled biphoton states in a fully integrated way, by using a single periodic waveguide and a single integrated pump mode. Moreover, in our proposal, one has access to all the phase-matching configurations of Figs. 1(a)–1(c) by only controlling the sign of the group velocity of the signal

and idler modes through dispersion engineering. We can control the extent of the entanglement in the generated states by varying geometry parameters without compromising their purity, enabling creation of Bell states and nonmaximally entangled states [46]. Furthermore, the ability to create and control entanglement in multiple degrees of freedom, such as spectrum, mode, and direction of propagation in our work, allows for the generation of hyper-entangled states [47], which are a valuable resource for quantum communication protocols. Obtaining counter-propagating phase matching without periodic poling is of high interest also in classical nonlinear applications, e.g., for realizing mirrorless optical parametric oscillators [48]. Finally, we emphasize that although we presented the general idea and the specific design using SPDC in a lithium niobate PCSW, the idea can be potentially extended to pair generation through SFWM in $\chi^{(3)}$ crystals.

We acknowledge financial support by the Carl Zeiss Foundation, the German Academic Exchange Service DAAD (PPP 57218492), and the German Federal Ministry of Education and Research (FKZ 03ZZ0434).

*sina.saravi@uni-jena.de

[1] M. A. Nielsen and I. L. Chuang, *Quantum Computation and Quantum Information* (Cambridge University Press, Cambridge, England, 2010).
[2] J. L. O'Brien, A. Furusawa, and J. Vučković, Nat. Photonics **3**, 687 (2009).
[3] S. Tanzilli, A. Martin, F. Kaiser, M. P. De Micheli, O. Alibart, and D. B. Ostrowsky, Laser Photonics Rev. **6**, 115 (2012).
[4] A. Orieux and E. Diamanti, J. Opt. **18**, 083002 (2016).
[5] P. G. Kwiat, K. Mattle, H. Weinfurter, A. Zeilinger, A. V. Sergienko, and Y. Shih, Phys. Rev. Lett. **75**, 4337 (1995).
[6] S. Tanzilli, W. Tittel, H. De Riedmatten, H. Zbinden, P. Baldi, M. DeMicheli, D. B. Ostrowsky, and N. Gisin, Eur. Phys. J. D **18**, 155 (2002).
[7] P. J. Mosley, J. S. Lundeen, B. J. Smith, P. Wasylczyk, A. B. U'Ren, C. Silberhorn, and I. A. Walmsley, Phys. Rev. Lett. **100**, 133601 (2008).
[8] R. Horn, P. Abolghasem, B. J. Bijlani, D. Kang, A. S. Helmy, and G. Weihs, Phys. Rev. Lett. **108**, 153605 (2012).
[9] A. Orieux, A. Eckstein, A. Lemaitre, P. Filloux, I. Favero, G. Leo, T. Coudreau, A. Keller, P. Milman, and S. Ducci, Phys. Rev. Lett. **110**, 160502 (2013).
[10] D. Kang, L. G. Helt, S. V. Zhukovsky, J. P. Torres, J. E. Sipe, and A. S. Helmy, Phys. Rev. A **89**, 023833 (2014).
[11] F. Setzpfandt, A. S. Solntsev, J. Titchener, C. W. Wu, C. Xiong, R. Schiek, T. Pertsch, D. N. Neshev, and A. A. Sukhorukov, Laser Photonics Rev. **10**, 131 (2016).
[12] K.-H. Luo, H. Herrmann, S. Krapick, B. Brecht, R. Ricken, V. Quiring, H. Suche, W. Sohler, and C. Silberhorn, New J. Phys. **17**, 073039 (2015).
[13] X. Li, P. L. Voss, J. E. Sharping, and P. Kumar, Phys. Rev. Lett. **94**, 053601 (2005).
[14] K.-i. Harada, H. Takesue, H. Fukuda, T. Tsuchizawa, T. Watanabe, K. Yamada, Y. Tokura, and S.-i. Itabashi, Opt. Express **16**, 20368 (2008).
[15] S. Azzini, D. Grassani, M. J. Strain, M. Sorel, L. G. Helt, J. E. Sipe, M. Liscidini, M. Galli, and D. Bajoni, Opt. Express **20**, 23100 (2012).
[16] C. Xiong, C. Monat, A. S. Clark, C. Grillet, G. D. Marshall, M. J. Steel, J. Li, L. O'Faolain, T. F. Krauss, J. G. Rarity, and B. J. Eggleton, Opt. Lett. **36**, 3413 (2011).
[17] N. Matsuda, H. Takesue, K. Shimizu, Y. Tokura, E. Kuramochi, and M. Notomi, Opt. Express **21**, 8596 (2013).
[18] D. Cruz-Delgado, R. Ramirez-Alarcon, E. Ortiz-Ricardo, J. Monroy-Ruz, F. Dominguez-Serna, H. Cruz-Ramirez, K. Garay-Palmett, and A. B. U'Ren, Sci. Rep. **6**, 27377 (2016).
[19] M. F. Saleh, B. E. A. Saleh, and M. C. Teich, Phys. Rev. A **79**, 053842 (2009).
[20] W. P. Grice, A. B. U'Ren, and I. A. Walmsley, Phys. Rev. A **64**, 063815 (2001).
[21] A. B. U'Ren, K. Banaszek, and I. A. Walmsley, Quantum Inf. Comput. **3**, 480 (2003).
[22] C. Monat, M. Ebnali-Heidari, C. Grillet, B. Corcoran, B. Eggleton, T. White, L. O'Faolain, J. Li, and T. Krauss, Opt. Express **18**, 22915 (2010).
[23] T. F. Krauss, Nat. Photonics **2**, 448 (2008).
[24] M. J. A. deDood, W. T. M. Irvine, and D. Bouwmeester, Phys. Rev. Lett. **93**, 040504 (2004).
[25] W. T. M. Irvine, M. J. A. deDood, and D. Bouwmeester, Phys. Rev. A **72**, 043815 (2005).
[26] M. Corona and A. B. U'Ren, Phys. Rev. A **76**, 043829 (2007).
[27] J. Li, T. P. White, L. O'Faolain, A. Gomez-Iglesias, and T. F. Krauss, Opt. Express **16**, 6227 (2008).
[28] A. Yariv and P. Yeh, J. Opt. Soc. Am. **67**, 438 (1977).
[29] R. Iliew, C. Etrich, T. Pertsch, F. Lederer, and Y. S. Kivshar, Phys. Rev. A **81**, 023820 (2010).
[30] A. S. Solntsev and A. A. Sukhorukov, Rev. Phys. **2**, 19 (2017).
[31] J. B. Spring, B. J. Metcalf, P. C. Humphreys, W. S. Kolthammer, X.-M. Jin, M. Barbieri, A. Datta, N. Thomas-Peter, N. K. Langford, D. Kundys, J. C. Gates, B. J. Smith, P. G. R. Smith, and I. A. Walmsley, Science **339**, 798 (2013).
[32] M. C. Booth, M. Atatüre, G. Di Giuseppe, B. E. A. Saleh, A. Sergienko, and M. C. Teich, Phys. Rev. A **66**, 023815 (2002).
[33] A. De Rossi and V. Berger, Phys. Rev. Lett. **88**, 043901 (2002).
[34] S. Ramelow, L. Ratschbacher, A. Fedrizzi, N. K. Langford, and A. Zeilinger, Phys. Rev. Lett. **103**, 253601 (2009).
[35] A. Christ, A. Eckstein, P. J. Mosley, and C. Silberhorn, Opt. Express **17**, 3441 (2009).
[36] V. Pasiskevicius, G. Strömqvist, F. Laurell, and C. Canalias, Opt. Mater. **34**, 513 (2012).
[37] C. Canalias, V. Pasiskevicius, M. Fokine, and F. Laurell, Appl. Phys. Lett. **86**, 181105 (2005).
[38] Z. D. Walton, A. V. Sergienko, B. E. A. Saleh, and M. C. Teich, Phys. Rev. A **70**, 052317 (2004).
[39] L. Lanco, S. Ducci, J.-P. Likforman, X. Marcadet, J. A. W. vanHouwelingen, H. Zbinden, G. Leo, and V. Berger, Phys. Rev. Lett. **97**, 173901 (2006).

[40] J. Monroy-Ruz, K. Garay-Palmett, and A. B. U'Ren, New J. Phys. **18**, 103026 (2016).
[41] See Supplemental Material at http://link.aps.org/supplemental/10.1103/PhysRevLett.118.183603 for the calculation of the biphoton state.
[42] Z. Yang, M. Liscidini, and J. E. Sipe, Phys. Rev. A **77**, 033808 (2008).
[43] S. Saravi, S. Diziain, M. Zilk, F. Setzpfandt, and T. Pertsch, Phys. Rev. A **92**, 063821 (2015).
[44] J. E. Sipe, N. A. R. Bhat, P. Chak, and S. Pereira, Phys. Rev. E **69**, 016604 (2004).
[45] K. Cui, Y. Huang, G. Zhang, Y. Li, X. Tang, X. Mao, Q. Zhao, W. Zhang, and J. Peng, Appl. Phys. Lett. **95**, 191901 (2009).
[46] A. G. White, D. F. V. James, P. H. Eberhard, and P. G. Kwiat, Phys. Rev. Lett. **83**, 3103 (1999).
[47] P. G. Kwiat, J. Mod. Opt. **44**, 2173 (1997).
[48] C. Canalias and V. Pasiskevicius, Nat. Photonics **1**, 459 (2007).